Available online at www.sciencedirect.com

SCIENCE DIRECT®

Tectonophysics 411 (2005) 1–18

TECTONOPHYSICS

www.elsevier.com/locate/tecto

A general framework for the occurrence and faulting of deformation bands in porous granular rocks

R.A. Schultz[a,*], R. Siddharthan[b]

[a] Department of Geological Sciences and Engineering, University of Nevada, Reno NV 89557, USA
[b] Department of Civil and Environmental Engineering, University of Nevada, Reno NV 89557, USA

Received 18 February 2005; received in revised form 23 July 2005; accepted 28 July 2005
Available online 9 November 2005

Abstract

Deformation bands form in porous granular rocks by localized inelastic yielding that is well described by a modified Cam cap model. All five kinematic varieties of bands observed in the field, including dilation bands, dilation bands with shear, shear bands, compaction bands with shear, and compaction bands, can be explained by this unifying mechanical framework once their localization criteria are also specified. The growth of dilation bands with shear has been observed in the field and in the laboratory for low-pressure conditions. More commonly, however, strain hardening of compaction bands with shear will lead to faulting within, and eventually through, the resulting damage zone if the associated yield cap grows outward sufficiently to intersect the frictional strength surface. This sequence is best explained by replacing the critical state line with a frictional failure criterion in the general Cam cap approach. Given recent advances in localization theory and continuing refinement of field observations, the term “fracture” must now be expanded to include both weak and strong discontinuities, or deformation bands and displacement discontinuities (i.e., cracks, joints, veins, solution surfaces, anticracks, dikes, sills, faults), respectively. Shear zones and fault zones that accommodate both continuous and discontinuous changes in shear offset within them should also be considered as *fractures* according to this expanded definition.

Keywords: Deformation bands; Yield caps; Critical state; Faulting

1. Introduction

Deformation bands are an important class of strain localization that occur in a wide variety of rock types, including sandstones, limestones, siltstones, poorly welded volcanic tuffs, and breccias (e.g., Aydin, 1978; Antonellini et al., 1994; Wilson et al., 2003; Evans and Bradbury, 2004). They may also occur in poorly indurated (“soft”) sedi-

* Corresponding author. R.A. Schultz can be contacted at: Tel.: +1 775 784 7318; fax: +1 775 784 1833. R. Siddharthan can be contacted at: Tel.: +1 775 784 1411; fax: +1 775 784 1390.
E-mail addresses: schultz@mines.unr.edu (R.A. Schultz), siddhart@unr.edu (R. Siddharthan).
URLs: www.mines.unr.edu/geo-engg/schultz (R.A. Schultz), unr.edu/homepage/siddhart/my_page.html (R. Siddharthan).

0040-1951/$ - see front matter © 2005 Elsevier B.V. All rights reserved.
doi:10.1016/j.tecto.2005.07.008

ments (e.g., Maltman, 1984, 1988, 1994; Du Bernard et al., 2002). The compactional and/or cataclastic variety of deformation bands commonly forms seals and impediments to fluid flow in these rock types (e.g., Crawford, 1998; Shipton et al., 2002; Vajdova et al., 2004a,b) and creates distributed networks called "damage zones" (e.g., Fossen and Hesthammer, 2000; Shipton and Cowie, 2003; Kim et al., 2004) that can later fail to form large-displacement faults (Aydin and Johnson, 1978).

Much of the standard literature on rock deformation and fault formation centers on Coulomb frictional sliding on a preexisting "zone of weakness" such as cracks and joints (e.g., Segall and Pollard, 1983b; Martel and Pollard, 1989; Reches and Lockner, 1994). While this approach may be relevant to faulting in crystalline rocks having very low porosity, such as granite, basalt, welded tuff, and high-grade metamorphic rocks, it does not adequately describe the faulting process in e.g., sedimentary rocks having higher porosities, as are commonly found in continental interiors and at plate margins (such as accretionary prisms and continental rifts). A considerable amount of theoretical work exists on the localization and development of deformation bands and faulting in these rocks (e.g., Rudnicki and Rice, 1975; Rudnicki, 1977; Aydin and Johnson, 1983; Issen and Rudnicki, 2000; Bésuelle and Rudnicki, 2004; Borja and Aydin, 2004; Borja, 2004; Aydin et al., in press) which provides a firm foundation for understanding these important structures. That work relies on a mathematically rigorous theory of band localization that predicts where in the deformation process the host rock's properties bifurcate into a two-phase medium consisting of less-deformed host rock plus highly deformed bands. In this paper we synthesize the results of much of this work, along with recent field results, using Cam cap models of yielding that are now widely employed in the deformation band literature (e.g., Antonellini et al., 1994; Cuss et al., 2003; Borja and Aydin, 2004; Borja, 2004; Wong et al., 2004; Aydin et al., in press; Wibberley et al., in press). This approach provides a simple yet powerful unifying framework for understanding the genesis and developmental sequence of deformation bands, damage zones, and attendant faulting.

A porous rock is defined here, following current usage (e.g., Zhu and Wong, 1997), as one that has greater than ~5% porosity. A crystalline rock has a negligibly small porosity. The larger porosity that is so characteristic of many poorly cemented and lithified sandstones, limestones, volcanic tuffs, and many limestones, breccias, and "soft sediments," drives a different style of deformation than commonly found for crystalline rocks like Westerly granite or various basalts. These crystalline igneous rocks have porosities that are so small (e.g., <<1%; Goodman, 1989, p. 29) that they behave as solid crystalline aggregates.

Porous rocks deform and localize zones of potential shearing in a very different fashion than do low-porosity crystalline rocks (e.g., Wong et al., 1992, 1997, 2004; Menéndez et al., 1996; Zhu and Wong, 1997; Johnson, 2001). The key difference in behavior between these two fundamental types of rock is that cracking in a crystalline rock (i.e., moving the grains apart) requires less energy than does shearing (e.g., Aydin, 2000). In a porous granular rock, grains shift (i.e., shear, dilate, or compact) around by rearranging their packing and by grain-size reduction by crushing of the individual grains (Aydin and Johnson, 1978; Zhang et al., 1990). This shifting of grains in a porous rock leads to "yielding" (e.g., Khan et al., 1991) which is identified with the nucleation, or formation, of the kinematic classes of deformation bands identified by Aydin (2000), Du Bernard et al. (2002), and Bésuelle (2001a,b), among others, as long as certain additional criteria for band localization are met. As a result, the crystalline rock creates joints, as preexisting "planes of weakness," before it faults (i.e., slides frictionally; e.g., Segall and Pollard, 1983b; Martel and Pollard, 1989; Crider and Peacock, 2004), or it creates microcrack swarms that form the weak zone of shear as an earlier part of the same deformation event (e.g., Rudnicki, 1977; Lockner et al., 1991; Moore and Lockner, 1995). In both cases, the deformation of crystalline rock involves dilatant cracks and local volume increase that subsequently shears (e.g., Reches and Lockner, 1994).

Faulting of a zone of deformation bands is defined as the *superposition of an array of linked slip patches, formed by Coulomb frictional sliding, onto the pre-existing or precursory zone, forming a surface of displacement discontinuity through the zone* (Schultz, in press). Because shearing of crystal grains is more difficult than dilatancy when the host-rock porosity is small, mode-II faults are unable to propagate in-plane through a crystalline rock as "shear cracks" (e.g., Petit and Barquins, 1988). Instead, faulting typically occurs only after a zone of deformation bands or other types of localized strain (e.g., Flodin and Aydin, 2004) already exists (e.g., Aydin and Johnson, 1978, 1983; Shipton and Cowie, 2001, 2003; Schultz and Balasko, 2003). As a result, faulting corresponds mechanically to "failure," rather to initial yielding of the rock.

This dichotomy in response as a function of rock porosity is probably the main reason why a distinction is often drawn in the literature between what have classically been called "fractures" (cracks and faults in crystalline rocks) and deformation bands (as formed in porous rocks). However, this distinction is not particularly useful or necessary anymore, since cracks, faults, and deformation bands (of all five kinematic types; Borja and Aydin, 2004) *function as fractures*, or discontinuities, within the deforming rock mass (e.g., Aydin and Johnson, 1983; Du and Aydin, 1993; Schultz and Balasko, 2003; Okubo and Schultz, 2005, in press; Schultz, in press). Indeed, the conditions for localization of either type of discontinuity in a pressure-sensitive, dilatant/frictional material are quite similar, as discussed by Borja (2002) and more recently, by Aydin et al. (in press). Bands having a continuous change in normal or shear strain across them (by definition) are predicted by an increase in the displacement gradient in the host rock (analogous to a classically defined shear zone, called a "weak discontinuity" by e.g., Borja, 2002; see also Crouch and Starfield, 1983, pp. 208–210). On the other hand, cracks and faults are associated with a step-wise change in the displacement distribution, leading to the terms "displacement discontinuity" (e.g., Crouch and Starfield, 1983, pp. 80–84; Pollard and Aydin, 1988) and "strong discontinuity" (Borja, 2002; Aydin et al., in press). In the limit of zero band thickness, a shear deformation band would be considered to become instead a slip patch (Aydin et al., in press). As a result, the generic term "fracture" should be expanded to include both weak and strong discontinuities; that is, both deformation bands (of any of the five kinematic varieties as discussed in Section 3.1) and the classical displacement discontinuities (i.e., cracks, joints, veins solution surfaces, anticracks, dikes, sills, faults; Pollard and Segall, 1987). Shear zones and faults zones that accommodate both continuous and discontinuous changes in shear offset across them (e.g., Davatzes et al., 2005) should also be considered as fractures according to this expanded definition.

2. Deformation bands in the field

Many fine occurrences of deformation bands and their geometries are known from around the world (see recent reviews and discussion of several of these by Fossen and Hesthammer, 1997; Davis, 1999; Shipton and Cowie, 2001, 2003; Borja and Aydin, 2004). Some examples of geometries in outcrop that are representative of strain-hardening cataclastic deformation band networks are shown in Fig. 1. Deformation bands in highly porous rocks (porosity exceeding ~15%) tend to form in spaced arrays of parallel bands a few mm thick that may define conjugate or orthogonal (Aydin and Reches, 1982; Shipton and Cowie, 2001) networks (Fig. 1a). Bands also tend to cluster in closely spaced zones, either in response to strain hardening within the bands (e.g., Aydin and Johnson, 1978) or perhaps to continued in-plane propagation of bands beyond their stepovers (e.g., Okubo and Schultz, in press), forming thicker zones several cm thick. These band zones can bound spaced arrays within damage zones (Fig. 1b; Davis, 1999) within which linking bands nucleate and grow (Schultz and Balasko, 2003).

The growth and geometry of deformation band stepovers (including the interior linking bands), arrays, and damage zones have recently been explored and successfully simulated in mechanical analyses of band growth by using strain energy density (e.g., Du and Aydin, 1993; Schultz and Balasko, 2003; Okubo and Schultz, 2005, in press). This approach utilizes a plastic yield criterion analogous to the von Mises criterion used in metals and geomaterials where pressure-independent deformation occurs (e.g., Jaeger, 1969, pp. 92–93; Jaeger and Cook, 1979, pp. 229–230; Davis and Selvadurai, 2002). Strain energy density is suitable for describing band growth on the Cam yield surface. Okubo and Schultz (2005) have demonstrated that band nucleation, associated with a local increase (for dilation bands) or decrease (for compac-

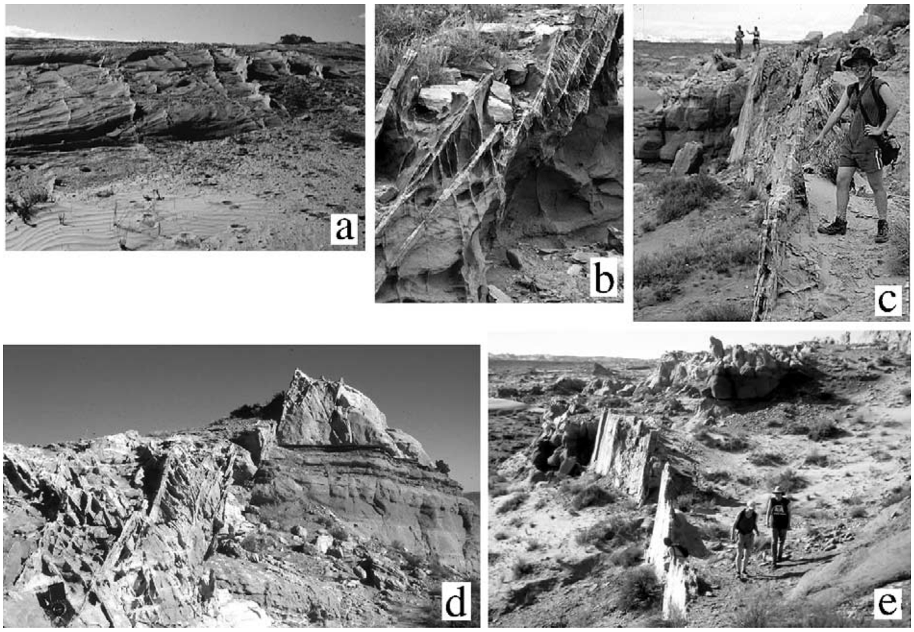

Fig. 1. Field expression of representative (cataclastic compaction with shear) deformation band arrays. Sense of shearing offset is normal (left side down in (b–e)) in all panels. (a) Conjugate sets of individual unfaulted deformation bands (resistant fin-like surfaces) in eolian Entrada Sandstone of southeast Utah (Fossen and Hesthammer, 1997). (b) Spaced array of linked bands (Davis et al., 2000; Schultz and Balasko, 2003) corresponding to an unfaulted damage zone ~1–2 m wide. (c) Faulted zone of deformation bands in (Aydin and Johnson, 1978) showing relict damage zone architecture in exposed footwall. (d) Faulted zone of deformation bands >4 m wide showing the through-going fault surface slicing through the interior of the damage zone (Schultz and Fossen, 2002). (e) Same locality as (c) showing corrugations in the fault surface that were inherited from the previously formed deformation band array (Schultz and Balasko, 2003).

tional bands) in porosity can be predicted by calculating the volumetric strain energy density, whereas shear band propagation and linkage can be evaluated by calculating distortional strain energy density (Du and Aydin, 1993; Schultz and Balasko, 2003; Okubo and Schultz, 2005, in press).

Slip patches can be identified as small smooth polished surfaces along zones of bands perhaps 5 mm thick (e.g., Shipton and Cowie, 2001; Schultz and Balasko, 2003). Faulting of band zones proceeds in two stages. First, slip patches nucleate on the previously formed band zone, inheriting its geometry (e.g., Aydin and Johnson, 1978; Antonellini et al., 1994; Davis, 1999; Shipton and Cowie, 2001; Schultz and Balasko, 2003; Fig. 1c, e). Next, linkage of slip patches produces a through-going fault within the damage zone (e.g., Shipton and Cowie, 2003; Fig. 1c and d). The field relations support a switch from a distributed strain-hardening regime during cataclastic band growth to a focused strain-softening regime during faulting.

3. Yield and failure of a porous rock

The basic approach to understanding the occurrence (localization) of deformation bands draws from the application of soil mechanics to porous rock deformation (e.g., Rudnicki and Rice, 1975; Rudnicki, 1977; Vermeer and de Borst, 1984; Wong et al., 1992, 2004; Bésuelle and Rudnicki, 2004). The porous rock is loaded until it begins to yield, defined as a transition from elastic to permanent (plastic) deformation (e.g., Rudnicki, 1977; Khan et al., 1991). Precisely how it yields (e.g., what kind of band forms) depends on the host-rock's porosity, grain packing geometry (Antonellini and Pollard, 1995), pore-water content, depth of burial (i.e., confining pressure), the differential stress that drives the deformation, and the stress path that the rock has taken to get from its undeformed state to its yielding state (e.g., Wong et al., 1992, 1997, 2004; Issen and Challa, 2003; Aydin et al., in press).

Researchers and practitioners in this field use a variant of the Mohr diagram, called a "q–p diagram" (Muir Wood, 1990, pp. 112–118; Antonellini et al., 1994; Nova and Lagioia, 2000; Davis and Selvadurai, 2002, pp. 68–71; Fig. 2). This approach is also referred to as a two-invariant model because each coordinate axis corresponds to a stress invariant. The three principal-stress invariants are (Davis and Selvadurai, 2002, p. 16).

$$I_1 = \sigma_1 + \sigma_2 + \sigma_3 \tag{1a}$$

$$I_2 = \sigma_1\sigma_2 + \sigma_2\sigma_3 + \sigma_1\sigma_3 \tag{1b}$$

$$I_3 = \sigma_1\sigma_2\sigma_3 \tag{1c}$$

The horizontal axis of the q–p diagram is $p = I_1$, the first stress invariant, identified as the mean stress, rather than just the normal stress (e.g., in a direct shear test) on a particular plane (on the Mohr diagram). The vertical axis is (Davis and Selvadurai, 2002, p. 57).

$$q = \sqrt{I_1^2 - 3I_2} \tag{2}$$

which reduces to $q = (\sigma_1 - \sigma_3)$, the differential deviatoric stress, for the particular two-dimensional case in which $\sigma_2 = \sigma_3$. The value of q equals the diameter of the Mohr circle and provides a measure of the shear stress supported in the rock (Davis and Selvadurai, 2002, p. 47) at the given value of mean stress p. The stresses are defined as effective stresses to include the important role of pore-water pressure in rock yield and failure; although primes are sometimes used in the literature in labeling the axes, they are not required (nor are they used in this paper) given the understanding that effective stresses are used in their calculation. The q–p diagram is much less cumbersome, and more informative, to use than the Mohr diagram

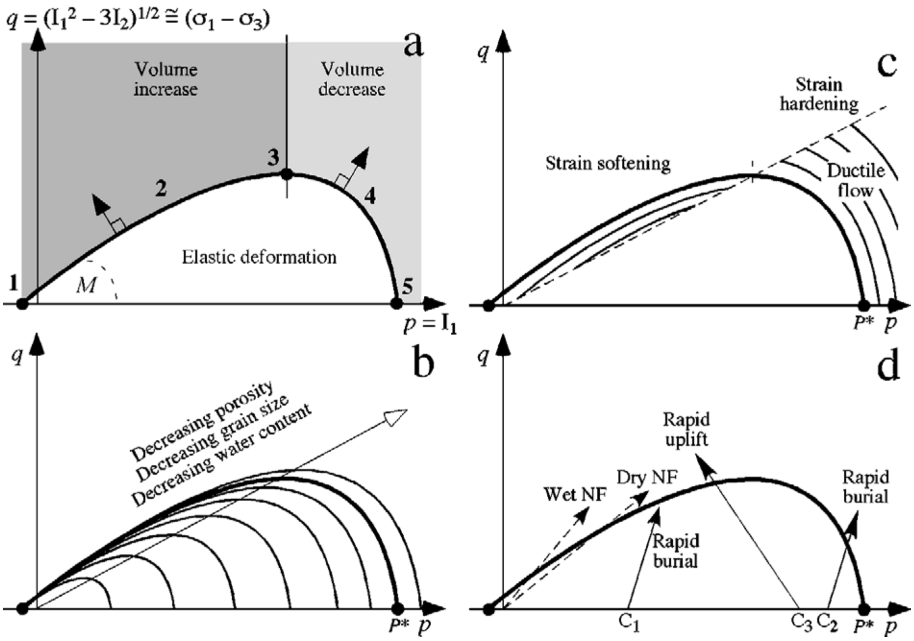

Fig. 2. Basic elements of the q–p diagram applied to porous rocks. (a) Cam yield surface (bold curve) with slope M showing approximate regions of deformation band nucleation (numbered, see text). Normal vectors to yield surface (see text for associated vs. noncoaxial flow laws) point to lower p for shear-induced dilation (dark shading) and to higher p for shear-enhanced compaction (light shading). (b) Yield surface expands for decreasing host-rock porosity, decreasing average grain size, and/or decreasing water content. P^*, grain crushing pressure. (c) Movement of yield surface is inward toward critical state line (dashed) for strain softening deformation; cap moves outward toward critical state line for strain hardening deformation. (d) Representative loading paths with arrows showing direction of progressive loading. Dashed lines, normal faulting regime for hydrostatic pore-fluid conditions in the crust ("wet NF;" $\sigma_1/\sigma_3 = 3$; see Suppe, 1985, p. 185) and anhydrous conditions ("wet NF;" $\sigma_1/\sigma_3 = 2$); rapid burial, increasing σ_1 from $\sigma_1 = \sigma_2 = \sigma_3$ (two different initial confining pressures C_1 and C_2 are shown); rapid uplift, decreasing σ_1 from $\sigma_1 = \sigma_2 = \sigma_3$ (initial confining pressure C_3).

because it facilitates tracking of two-dimensional or three-dimensional loading (stress) paths that the rock takes to yielding and then to failure in a porous rock without well-defined weakness zones, and it also makes more sense on the high-pressure "yield cap" side (Risnes, 2001). The q–p diagram is found in much of the literature on band formation in porous rocks (e.g., Antonellini et al., 1994; Wong and Baud, 1999; Baud et al., 2004; Borja and Aydin, 2004; Wong et al., 2004).

The locus of stress states that separates the elastic from the inelastic yielding regimes is called a "yield surface" (e.g., Schofield and Wroth, 1968; Muir Wood, 1990; Khan et al., 1991; Davis and Selvadurai, 2002). The shape of the yield surface shown in Figs. 2 and 3 depends on the physical characteristics of the porous rock being deformed (e.g., Wong et al., 1992; Issen and Rudnicki, 2000; Borja and Aydin, 2004; Borja, 2004). At lower confining pressures, the yield surface has a positive slope where shear bands with dilatancy are formed ("dilatant shear" and dark shading in Fig. 2a). At higher confining pressures (i.e., at greater depths), the yield surface has a negative slope where shear bands with compaction are formed ("compactional shear" and light shading in Fig. 2a, called the "cap").

The yield surface does not need to intersect at the origin (i.e., for a tensile mean stress; Wong et al., 1997; Borja and Aydin, 2004; Borja, 2004). At the other, high-pressure extreme, the yield surface (cap) intersects the mean-stress axis p (having zero shear stress there) at a point called the grain crushing pressure, P^* (e.g., Wong et al., 1992, 1997). This is the pressure at which any of compaction, grain crushing, and/or volume loss occur in the absence of shearing (i.e., isotropic or "hydrostatic" loading). This important value scales approximately with the product of average grain size R and porosity Φ, which is approximated for spherical, monolithologic grains (but good to first order for other grain size distributions; Wong et al., 2004) by (Zhang et al., 1990; Wong et al., 1997)

$$P^* = (\Phi R)^{-1.5}. \tag{3}$$

As a result, a series of yield surfaces can be drawn for rocks of different porosities and grain sizes (Fig. 2b). As grain size increases, porosity increases, or both, the grain crushing pressure decreases (moves to the left on Fig. 2b) and so does the size of the yield surface (Fig. 2b). On the other hand, as porosity goes to zero for a crystalline rock like a granite, basalt, or

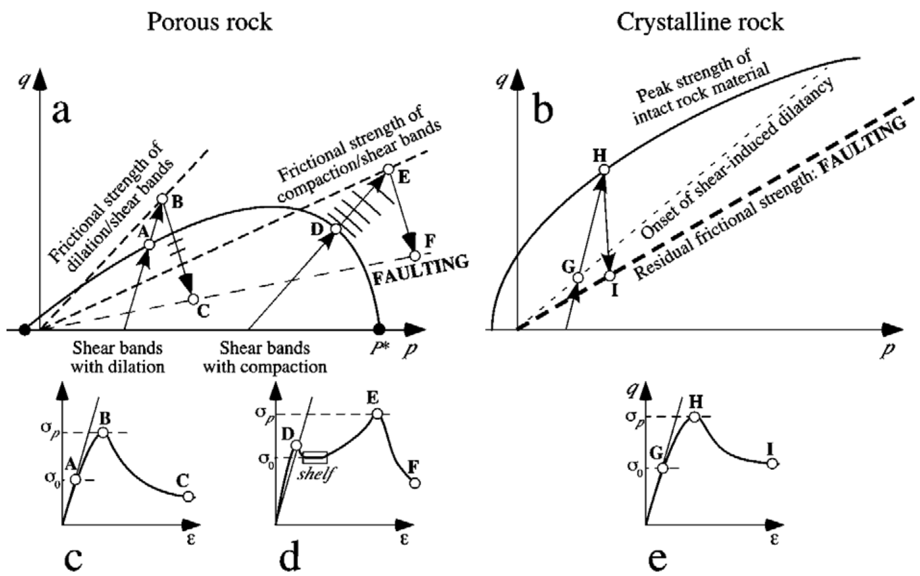

Fig. 3. Comparison of fault growth in (a) porous rock (porosity > 5%) and (b) crystalline rock (porosity << 5%) for a compressive remote stress state. Lettered stress paths in (a) correspond to the stress–strain diagrams in (c), for dilatant shear bands, and (d), for compactional (i.e., cataclastic) shear bands. The stress path in (b) corresponds to the stress–strain diagram for crystalline rock in (e). Dashed gray lines in (a) depict yield surfaces moving toward the frictional sliding line.

quartzite, the grain crushing pressure theoretically goes to infinity, meaning that it is no longer a relevant property of a low-porosity rock. The water content of a porous rock also influences its yield surface. The yield surface contracts in size, while retaining the same shape, as the water content increases (e.g., Wong and Baud, 1999; Wong et al., 1992), as illustrated in Fig. 2b.

The yield surface shown in Figs. 2 and 3 is one of a class that includes "Modified Cam Clay" (Roscoe et al., 1958, 1963; Roscoe and Poorooshasb, 1963; Roscoe and Burland, 1968), named after the Cam River at Cambridge, England, where the original work on plastic yielding of clay-rich and granular soils was done (Wood, 1990, p. 113; Davis and Selvadurai, 2002, p. 70). Clear expositions of this technique are given by Schofield and Wroth (1968), Muir Wood (1990), pp. 112–138, and Davis and Selvadurai (2002), pp. 190–210. The dilational side of the yield surface (see Fig. 2a) is called the "Hvorslev surface" in soil mechanics (e.g., Farmer, 1983, pp. 90–94). It is analogous to a set of frictional sliding curves that track the material's water content (Schofield and Wroth, 1968, pp. 207–215) and physical state as it yields inelastically toward the critical state line. Because the elastic limit (corresponding to the Hvorslev part of the yield surface) and peak strength (corresponding to the frictional or critical-state line, discussed below) can be close in magnitude in soils, identification of the Hvorslev surface with either yielding or peak strengths in soils can be difficult or ambiguous. Recent work on porous rock shows, in contrast, a clearer separation between the yield and peak strengths (Okubo and Schultz, submitted for publication). The compactional side of the yield surface in soils, called the "yield cap" (e.g., DiMaggio and Sandler, 1971; Fig. 2c), is denoted the "Roscoe surface" (Farmer, 1983, pp. 90–94). These two surfaces meet along the critical state line.

In soil mechanics, the "critical state line" (e.g., Schofield and Wroth, 1968; Farmer, 1983; Muir Wood, 1990, pp. 139–213) reflects large shear deformation of the soil with no volume change. The critical state line (dashed diagonal line in Fig. 2c and d) separates the two fields of the yield surface discussed above: volume increase to the left and volume reduction to the right (see Fig. 2a). The slope M of this line on the q–p diagram (Fig. 2a) is related to the friction angle in pressure-sensitive soils and rocks (e.g., Jaeger and Cook, 1979) by (Muir Wood, 1990, p. 178)

$$M = \frac{6\sin\phi}{3 - \sin\phi} \tag{4}$$

and the friction coefficient $\mu = \tan\phi$.

A one-to-one correspondence between certain terms and concepts of Cam cap models for soils and rocks is not considered to be established. This is because homogeneous deformation and continuum flow are implied in critical state soil mechanics and the classical Cam cap model (T.-f. Wong, pers. comm., 2004), whereas strain localization is of more importance in rocks (e.g., Rudnicki and Rice, 1975; Wong et al., 1992, 2004; Bésuelle and Rudnicki, 2004). Consequently, the parts of the yield surfaces noted above are not referred to by the soil-mechanics names (i.e., Hvorslev, Roscoe surfaces, or the critical state line) in the context of porous rock deformation given that yielding may occur somewhat sooner than band localization in rock.

An important element in the interpretation of yield surfaces and caps for porous soil and rock is the "loading path" (e.g., Wong et al., 1992; Issen and Challa, 2003) which describes the rates of change of differential stress q and mean stress p taken by the soil or rock from its initial through final (yielded or faulted) deformation state. Many loading (or stress) paths are considered plausible for band nucleation in porous rock, including: (a) isotropic (hydrostatic) compression, corresponding to an increase in p at $q = 0$ (Fig. 2d); (b) triaxial test conditions, here called "rapid burial" on Fig. 2d, having constant p and increasing compressive σ_1; (c) constant σ_1 with increasing p (Issen and Challa, 2003); (d) constant σ_1 with decreasing p (Issen and Challa, 2003); (e) constant p and increasing compressive σ_1, here called "rapid uplift" on Fig. 2d; and (f) Coulomb friction with σ_1/σ_3=constant (i.e., $\sigma_1/\sigma_3 = 3$ for dry host rock or ~2 for water-saturated host rock).

Although loading paths are easily determined for laboratory experiments and theory, actual stress paths taken by naturally deformed rocks are difficult to assess (e.g., Wibberley et al., in press). Nevertheless, some general observations can be made. Dilation band with shear (see Fig. 2a, point 2 and next section) can be formed by any loading or unloading path (Fig. 2d) as long as the dilatant side of the yield surface (Fig. 2a, dark shading) is reached. Shear bands (Fig. 2a, point 3) can be reached by the non-Coulomb paths. Compaction bands with shear (Fig. 2a, point 4) apparently require triaxial or burial conditions from initially large values of confining pressure p, although a steep unloading path from larger initial p can also intersect the yield cap. Compaction bands imply large values of p (Fig. 2a, point 5), whereas dilation bands (Fig. 2a, point 1) imply small values of p.

3.1. Band habitats on the yield surface

In this section we present a summary of the varieties of deformation bands found in porous rocks and their significance for kinematics and mechanics. This kinematic classification scheme draws from current usage (e.g., Borja and Aydin, 2004; Aydin et al., in press) and highlights the importance of stress path on the type of band formed (i.e., where the yield surface is initially intersected by the stress state in the host rock).

A *dilation band* (Du Bernard et al., 2002; point 1 on Fig. 2a) accommodates separation of rock across its walls, with no shearing offsets, but differs from a mode-I crack by being filled with host rock having greater porosity than that outside the band. The kinematics of a dilation band are thus similar to those of cracks and dilation bands probably form in many of the same patterns (e.g., Segall and Pollard, 1983a; Pollard and Aydin, 1988). For example, they have recently been identified in the dilational quadrants of small thrust faults in poorly consolidated sands in coastal California (Du Bernard et al., 2002). Dilation bands were predicted theoretically (Issen and Rudnicki, 2000; Bésuelle, 2001b; Issen, 2002) and observed experimentally (Bésuelle, 2001a). These bands do not have cataclasis and likely serve as efficient conduits for fluid flow in the subsurface due to their enhanced porosity relative to the host rock.

Dilation bands with shear were predicted theoretically (e.g., Bésuelle, 2001b) and observed in experiments (Bésuelle, 2001a) and in the field (e.g., Antonellini et al., 1994; Borja and Aydin, 2004; Okubo and Schultz, 2005, submitted for publication). These bands appear to be rarer than the compactional varieties. They form to the left of the frictional sliding line on Figs. 2 and 3 (point 2 on Fig. 2a), but can also occur into the compactional side, depending on the properties of the deforming rock (Borja and Aydin, 2004). Like dilation bands, these bands should conduct fluids effectively and also lack cataclasis.

Shear bands (e.g., Wibberley et al., 1999; Fossen, 2000; Fisher et al., 2003; Borja and Aydin, 2004) accommodate shearing with no volume change (dilation or compaction) within the band. These bands occur near the top of the yield surface of Figs. 2 and 3 where its slope approaches zero (point 3 on Fig. 2a). Occasionally called “disaggregation bands” (e.g., Fossen, 2000), in detail the morphology of shear bands sometimes resembles a deforming layer of gouge, complete with a Riedel-like array of shear surfaces (e.g., Bartlett et al., 1981; Gu and Wong, 1994; Marone, 1995; Mair et al., 2000) within the band, depending on the magnitude of strain accommodated across it. These bands may be quite common and important in soft-sediment deformation.

Compaction bands with shear are the most commonly recognized “type example” of deformation band in porous rocks (point 4 on Fig. 2a; e.g., Aydin, 1978; Aydin and Johnson, 1978, 1983; Jamison and Stearns, 1982; Fossen and Hesthammer, 1997, 1998; Cowie and Shipton, 1998; Wibberley et al., 2000; Shipton and Cowie, 2001, 2003). Compaction, grain crushing, and porosity reduction in these bands contribute, individually or in combination, to strain hardening, and thus to creation of a spatially distributed network of bands called a “damage zone” that precedes faulting (e.g., Shipton and Cowie, 2003; Crider and Peacock, 2004; Kim et al., 2004). The bands also have significantly reduced permeability (e.g., Antonellini and Aydin, 1995; Shipton et al., 2002), producing seals to flow of groundwater and petroleum (e.g., Aydin, 2000; Shipton et al., 2005).

Compaction bands (point 5 on Fig. 2a) have been recognized in the field by Mollema and Antonellini (1996), in experiments by many including Olsson (1999), Olsson and Holcomb (2000), Wong et al. (2001) and Vajdova and Wong (2003), and theoretically by Issen and Rudnicki (2000, 2001), Olsson (2001), Bésuelle (2001b), Issen (2002), and Challa and Issen (2004). This is the other end-member of volumetric deformation bands (Borja and Aydin, 2004) that lack shear offsets (the first end-member is the dilation band). Compaction bands also form barriers to subsurface fluid flow (Holcomb and Olsson, 2003; Vajdova et al., 2004b) and can contribute to the creation of damage zones by growing in the contractional (leading) quadrant of nonconservative (mode-II) faults.

The term "deformation band" as used in the literature formally includes the three shear varieties (dilation and shear, shear, compaction with shear); the other two cases of normal strain across the band (dilation and compaction bands) are not called deformation bands in many parts of the literature. However, as we saw in the previous section and in Figs. 2 and 3, all five kinematic varieties of bands can be understood using the framework of a Cam cap model as applied to porous granular rocks, so all five varieties should be considered as "deformation bands" (e.g., Aydin et al., in press).

3.2. Deformation sequence

The formation of bands in porous soils and rocks is well documented and understood (e.g., Papamichos and Vardoulakis, 1995; Saada et al., 1999; Nova and Lagioia, 2000; Wolf et al., 2003; Wong et al., 2004). Suppose we take a sandstone or a limestone with, for example, 10% porosity, and start to apply differential stresses with a low confining pressure (e.g., in a triaxial test). Band localization depends in part on the porosity and grain packing geometry. As the rock compresses and starts to squeeze together, the stress–strain curve departs from linearity, marking the onset of inelastic deformation and yielding. The normal vector to the yield surface (see Fig. 2a) at the point where the stress path intersects it (e.g., point A on Fig. 3a and c) determines how the yield surface will move with increasing strain within the rock. If the vector points to the left, as it will in the dilatant shear regime (since the yield surface has a positive slope there), then the stress path and corresponding yield surface can move down toward the failure line (compare Fig. 2a and c; Wood, 1990, p. 124). Similarly, the vector points to the right for the yield cap (Fig. 2a), requiring that the surface of compactional yielding must expand upward toward the failure line (Fig. 2c), as shown in many experiments on porous rock (e.g., Wong and Baud, 1999; Cuss et al., 2003; Vajdova et al., 2004a).

Plastic yielding in soils and rocks is treated by assuming either associated or non-associated behavior during inelastic yielding (e.g., Vermeer and de Borst, 1984; Bésuelle and Rudnicki, 2004; Borja and Aydin, 2004). Associated flow rules assume coaxiality between remote stresses and the strains within the newly forming band (equivalent to the small-strain approximation; see Borja, 2002, for analysis and discussion), implying that the friction angle equals the dilatancy angle of the host rock. The dilatancy angle is defined as the ratio of plastic volume change to plastic shear strain (Vermeer and de Borst, 1984), or equivalently, as the slope of the plastic volume change vs. plastic shear strain curve on the q–p diagram (called in this case the "dilatancy factor"; Aydin and Johnson, 1983; Bésuelle, 2001a,b). Yield surfaces in the dilatant or compactional regimes contract or expand in the direction normal to their local slopes for associated plasticity (as shown in Fig. 2a). However, because the dilatancy angle is commonly different (usually smaller for the dilatant regime; Vermeer and de Borst, 1984) than the friction angle of soils, concrete, and porous rocks (Vermeer and de Borst, 1984), non-associated flow rules that assume non-coaxiality between remote stresses and strains within the bands are now routinely used (e.g., Wibberley et al., 1999; Wong et al., 2001, 2004; Issen and Challa, 2003; Bésuelle and Rudnicki, 2004; Borja and Aydin, 2004). In this case, the direction of local yield surface change will not be precisely perpendicular to the local slope, but the overall sense of yield surface migration (i.e., outward or inward) will be the same. Work reported by Issen and Rudnicki (2000), Borja and Aydin (2004), and Wong et al. (2004) suggests that growth of compaction and dilation bands is facilitated by an associated flow rule, whereas shear band growth (including the dilatant-shear and compactional-shear varieties) is facilitated by non-associated flow rules.

The Cam clay model was designed as an engineering tool to define the upper limit of elastic deformation of either normally consolidated or overconsolidated soils (corresponding to Fig. 3c and d, respectively). Conditions for localization of shear bands that form so commonly in soils during yielding (Papamichos and Vardoulakis, 1995; Saada et al., 1999; Davis and Selvadurai, 2002; Wolf et al., 2003) are therefore not specified by the standard two-invariant Cam clay model. As a result, three-invariant Cam clay models were developed (e.g., Perić and Ayari, 2002a,b) to more closely associate yielding with shear band localization in soils.

In porous rocks, deformation bands are considered to localize when a particular set of conditions is met. In general, band localization occurs when a parameter known as the "hardening modulus" (e.g., Rudnicki and Rice, 1975; Rudnicki, 1977; Aydin and Johnson, 1983; Bésuelle and Rudnicki, 2004) achieves a critical value. This parameter, defined as the local slope of the axial stress vs. plastic axial strain curve (e.g., Bésuelle, 2001a) depends on the elastic parameters of the host rock (shear modulus, Poisson's ratio), the dilatancy angle, the hardening modulus, and the local slope of the yield surface (equivalent to friction angle for the dilatant regime) at particular values of the stress state within the rock (Bésuelle and Rudnicki, 2004). All three stress invariants are needed to fully characterize the stress state at band localization (Bésuelle and Rudnicki, 2004). Because the remote stress state can be represented by a parameter called the Lode angle in soil plasticity (e.g., Hill, 1950), three-invariant Cam clay models that incorporate the Lode angle (Perić and Ayari, 2002a,b; Davis and Selvadurai, 2002) can be used to more accurately predict shear band localization in soils as plastic yielding is achieved. This approach is equivalent to, if less comprehensive than, contemporary theoretical research on the localization of all five varieties of deformation bands that can form in porous rocks (e.g., Borja and Aydin, 2004). The literature is vague on how different the stress conditions for yielding are from those required for band localization. Indeed, the available results suggest that yielding, in the form of significant grain reorganization, occurs in close physical and temporal proximity to a growing band or as part of the band itself. In either case (soil or porous rock), in this paper we take the onset of yielding as a reasonable first-approximation to the conditions associated with band localization.

Once the localization conditions are met, the elastic limit on the stress–strain curve for a porous rock corresponds to inelastic yielding, nucleation of dilatant shear bands, and a macroscopic strain softening behavior in the rock (point A in Fig. 3a and c). As the rock continues to soften with increasing strain, as shear-enhanced dilation occurs, the stress state moves toward the frictional sliding line, which represents the peak (maximum) frictional strength of the newly formed dilatant shear band. Discrete slip patches (e.g., Martel and Pollard, 1989) grow and frictional sliding along them begins between points B and C on Fig. 3a and c, representing strain softening due to dilatancy and increased volume within the rock. At this stage the band "fails in shear," producing a faulted dilatant shear band (points B and C on Fig. 3a and c). This process (up to faulting) has only recently been emphasized in experimental studies (Issen and Challa, 2003) and it deserves further work to clarify the details of band localization and growth. The deformation sequence has recently been identified in natural exposures of Wingate Sandstone (Okubo and Schultz, 2005) and produced experimentally (Cuss et al., 2003; Okubo and Schultz, submitted for publication).

If instead we load a porous rock sample starting at a much higher confining stress (for the same rock porosity and grain packing geometry), then after initial yielding we follow the path D–F on Fig. 3a and d. As we increase the differential stress and the rock begins to compress and shear, the grain-to-grain contacts experience a much larger compressive stress, leading in well sorted rocks (with a uniform grain size) to fracturing and grain crushing (Aydin, 1978; Zhang et al., 1990). This has the triple result of: (a) reducing the average grain size within a growing band, (b) producing a tighter packing geometry, and (c) making the grains more angular and consequently less able to roll under shear stress (Mair et al., 2002). These three factors all make it more difficult to accommodate shearing displacements within a band formed of such material; as a result, the band progressively strain hardens. Such compaction bands with shear form near point D on Fig. 3a and d, marking to the onset of inelastic yielding and volume reduction in the rock. However, because grain crushing depends on several factors including grain size and distribution, packing geometry, grain composition and shape (Antonellini and Pollard, 1995; Wong et al., 1997; Wong and Baud, 1999), the same stress state may produce compaction *without* cataclasis in one rock type (e.g., poorly sorted, matrix-supported) and compaction *with* cataclasis in another (e.g., well sorted, clast-supported).

There is commonly a region of the stress–strain curve for porous soils and rocks subjected to this higher confining pressure called a "shelf" (Fig. 3d). Here, strain accumulates under constant differential stress, indicating a plastic strain that corresponds to compaction within the rock (Wong et al., 1992; Olsson, 1999, 2001; Olsson and Holcomb, 2000; Nova and Lagioia, 2000; Issen, 2002). Stress–strain curves for this region that do not reach the point of failure (Fig. 3d, point E) are called "ductile" in the literature.

The width of the shelf (i.e., the amount of strain accommodated) is proportional to the amount of porosity reduction in the rock, so higher porosity rocks can have a longer shelf than do lower porosity rocks. In the limit of negligible porosity, the stress–strain curve for a crystalline rock will not show a shelf since there is no pore volume to collapse.

Once the compactional shear bands have formed and filled the available pore volume within them, the bands have become stiffer than the surrounding host rock. The stress–strain curve then increases with increasing strain because it is harder to deform this rock than it was for the undeformed (and more porous) host rock. The yield cap now represents the properties of the compactional shear band network (i.e., the damage zone within the host rock). Strain hardening expands the yield cap (e.g., Cuss et al., 2003), since the damage zone is strain *hardening* and because it is increasing in size relative to the volume of the host rock, until the stress state associated with frictional sliding between elements of the damage zone is achieved. If the yield cap and frictional-sliding line have different slopes at their intersection point, as is typical, then this point is called a "vertex." At the vertex (E on Fig. 3a and d), the frictional strength of the damage zone is reached, slip patches nucleate at the interfaces between the individual bands and the less-deformed rock (Aydin and Johnson, 1983), and grow within the damage zone (Aydin and Johnson, 1978; Johnson, 1995; Shipton and Cowie, 2001, 2003; Schultz and Balasko, 2003), eventually forming a through-going fault (point F on Fig. 3a and d). This sequence is the most thoroughly studied stress path in porous rocks and it is what most geologists think of when they encounter the term "faulted deformation band."

In contrast, as a crystalline rock (with negligible initial porosity) is loaded (Fig. 3b), the rock's elastic limit is reached where microcracking begins along with a shallowing of the slope of the stress–strain curve; this is point G on Fig. 3b and e. The rock softens until the cracks can grow by segment linkage into macrocracks, corresponding to the rock's peak strength (point H on Fig. 3b and e). Finally, the residual frictional strength of the inclined zone of linked cracks (Tapponier and Brace, 1976; Nemat-Nasser and Horii, 1982; Wong, 1982; Horii and Nemat-Nasser, 1985; Fredrich et al., 1989; Reches and Lockner, 1994) is met, leading to frictional sliding along the linked and abrading crack array and formation of a through-going fault (point I on Fig. 3b and e). The slope of this residual frictional sliding line is shallower than that for initial sliding on a rough discontinuous crack array near peak strength (e.g., Moore and Lockner, 1995).

As in the case of a porous rock, three surfaces are needed to describe how an intact crystalline rock finally forms a through-going fault. The first corresponds to the onset of inelastic dilatant yielding in the rock (Rudnicki, 1977; Wong, 1982; Khan et al., 1991; Lockner et al., 1991; Wong et al., 1997; Zhu and Wong, 1997). The second is the peak strength that represents failure of the rock as microcracks coalesce to form a linked array of macrocracks. The third is corresponds to residual frictional sliding along the linked crack array (the "fault"). At some (large) value of confining pressure, the rock is no longer able to open microcracks and produce dilatancy, so a fault would not localize in the way described (the rock's "brittle–plastic transition;" e.g., Wong et al., 1992). Non-localized distributed shearing (i.e., macroscopic flow) would occur in the rock at pressures exceeding this brittle–plastic transition.

A porous rock need not make a fault; the many examples of unfaulted deformation bands of all types (dilation, compaction, shear, dilation with shear, and compaction with shear) demonstrate that the process can and has been interrupted in nature at any stage along the stress path. In fact, it may take quite a bit of effort to get from point D to point E on Fig. 3a and d, which probably explains why we see so many examples of unfaulted cataclastic deformation bands (including arrays or damage zones that have only small, unlinked slip patches within them).

4. The brittle–ductile transition in porous rocks and faulted damage zones

In the rock mechanics literature, brittle deformation is associated with localized dilatancy and faulting, whereas ductile deformation is associated with nonlocalized macroscopic flow (e.g., Evans and Kohlstedt, 1995; Fig. 2c). The stress–strain curve for the brittle regime rises to a peak, then decreases in the post-peak region toward a residual (frictional) strength (e.g., Fig. 3c or e); the post-peak region is characterized by strain softening behavior and localization of strain onto discrete slip patches. On the q–p diagram, the brittle–ductile transition is commonly taken to be the intersection of the yield surface with the critical state line (e.g., Wong et al., 1992; Cuss et al., 2003; Fisher et al., 2003; Wibberley et al., in press), with brittle, localized deformation identified with the dilatant side (dark shading on Fig. 2a) and ductile flow with the compactional side (light shading on Fig. 2a). Strain softening and strain localization in the plastic regime, referred to as "high-pressure embrittlement" (e.g., Byerlee and Brace, 1969; Wong et al., 1992), can also lead to faulting, however. In this case, the peak strength (in the ductile or plastic regime; point E on Fig. 3d) occurs at sufficiently large values of differential stress q (or equivalently, large axial strain) that the post-peak region may not be revealed in a particular experiment or natural exposure. The rock may thus demonstrate only homogeneous macroscopic (ductile) flow and strain-hardening behavior, even if individual bands are localizing to form damage zones within the rock.

In the field, sets of compactional with shear deformation bands that demonstrate strain hardening along them (reduced porosity, grain size, and roundness; e.g., Aydin, 1978; Mair et al., 2000) group themselves into spaced arrays and damage zones (e.g., Aydin and Johnson, 1978; Davis, 1999; Shipton and Cowie, 2003; Fig. 1b). This stage represents the third step in forming a faulted zone of bands (after elastic strain and band nucleation), as outlined on Fig. 4. In this figure, the two peak strength envelopes (one for dilatant shear bands, one for compaction shear bands) have been replaced by a single curved envelope that may better represent the varying frictional strength of the band-host rock interface within the larger damage zone with increasing mean stress. Growth of the damage zone in size and complexity (Olsson and Holcomb, 2000; Wong et al., 2001; Olsson, 2001; Baud et al., 2004) is associated with a growing (expanding) yield cap on the q–p diagram (Fig. 4, step 3). Indeed, the region between band nucleation (step 2 on Fig. 4) and initial frictional failure of the band–host rock interface within the damage zone (step 4 on Fig. 4) represents macroscopic ductile flow (e.g., Cuss et al., 2003) in the damage zone (Fig. 2c).

Previous workers were mixed on the interpretation of the critical-state line as applied to porous rocks, defined in a soil as nonlocalized continuum flow. Summarizing previous work, Farmer (1983, pp. 91–93) reinterpreted critical state lines as equivalent to the Coulomb frictional strength of typical rocks (e.g., Byerlee, 1978; Lockner, 1995) and faults (Sibson, 1994) having σ_1/σ_3 ~3. Cuss et al. (2003) inferred that the critical state line was associated with distributed cataclastic flow within the sample, with faulting occurring later as a result of some unspecified "geometric forcing" constraint. Wibberley et al. (in press) infer the existence of a later tectonic event to reload a damage zone to failure. They noted that a fault cross-cuts the band network they studied, rather than being generated from slip patches that nucleated on bands within the network (e.g., Aydin and Johnson, 1978; Shipton and Cowie, 2001). Wibberley et al. suggest that the fully-formed fault represents deformation of the host rock at critical state. Most experimentalists and theorists investigate yielding (growth of band networks and damage zones) rather than failure (faulting of the damage zone) (e.g., Rudnicki and Rice, 1975; Bésuelle, 2001b; Issen, 2002; Wong et al., 2004; Bésuelle and Rudnicki, 2004; Aydin et al., in press). Aydin and Johnson (1983) analysis, in contrast, shows how bands can fail, nucleating small slip patches along them, for a sufficiently large contrast in (plastic) strain rate across the band–host rock interface. Their model appears most applicable to slip patch nucleation within a larger damage zone, as demonstrated in the field by Johnson (1995) and by Shipton and Cowie (2001, 2003) (point E on Fig. 3a, and step 4 on Fig. 4, corresponding to localized failure at peak strength at the "vertex").

Previous work demonstrates that the brittle–ductile transition in a soil, corresponding to the transition from localized (strain softening) to distributed (strain hardening) deformation, occurs where the slope of the yield surface on the q–p diagram becomes negative (Fig. 2c). We suggest in addition that the classical critical state line has little meaning when applied to porous rocks. Instead, lines defined by the peak (Fig. 4, step 4) and residual (Fig. 4, step 5) frictional resistance of deformation bands within the damage zone (Fig. 3a) define, respectively, the transition from distributed deformation within the expanding damage zone (the moving yield cap) to localized deformation

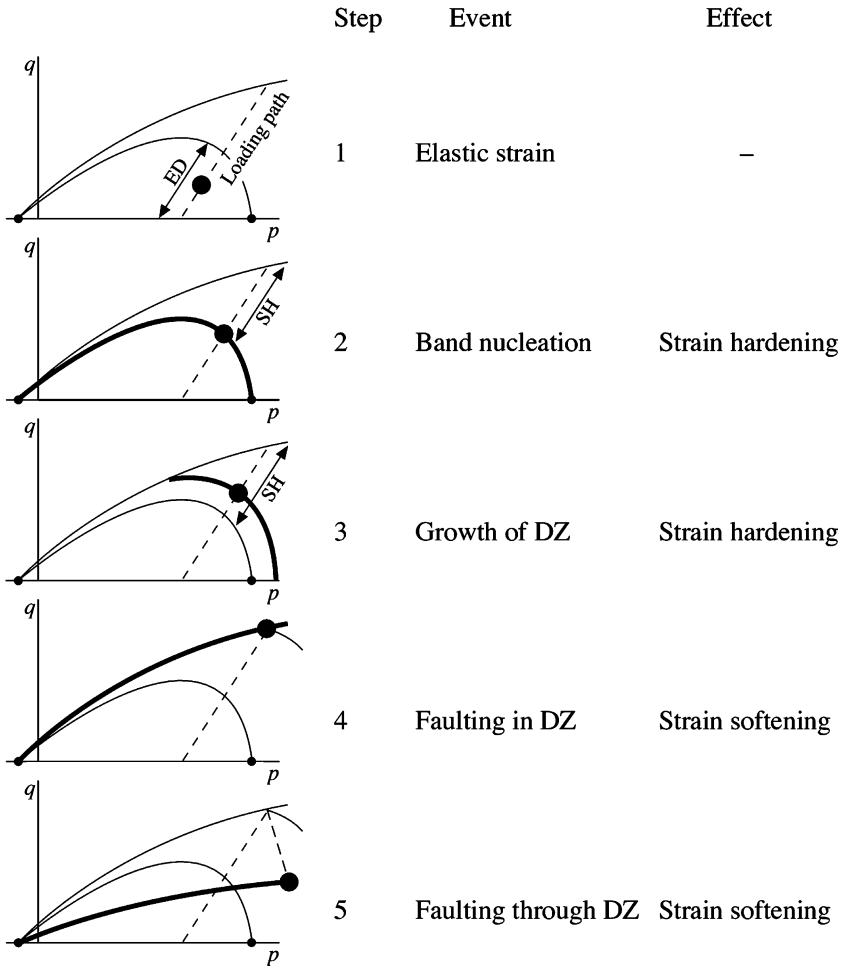

Fig. 4. Sequential development of a faulted array of compaction with shear deformation bands. ED, elastic deformation of host rock; SH, region of macroscopic strain hardening.

(faulting of bands), leading ultimately to failure of the damage zone by through-going faults.

A deformation sequence leading to faulted cataclastic band damage zones (point 4 on Fig. 2a) that is consistent with field observations, laboratory data, and theory is illustrated in Fig. 5. Following elastic straining of the host rock, individual deformation bands (specifically, compaction bands with shear) nucleate and grow in length and displacement (e.g., Aydin, 1978; Fossen and Hesthammer, 1997), forming a damage zone in the porous host rock when the stress state satisfies the yield cap (point D on Fig. 3a, step 2 on Figs. 4, 5a). The damage zone may be either spatially extensive across an outcrop, as illustrated in Figs. 1a and 5a (e.g., Fossen and Hesthammer, 1997), or it may define a narrower zone of mechanically interacting bands (Schultz and Balasko, 2003; Okubo and Schultz, 2005). As the damage zone grows in spatial extent and complexity (Fig. 5b), the yield cap moves outward, reflecting strain hardening of the zone (step 3 on Figs. 4, 1b, 5b). Localized failure (Aydin and Johnson, 1983), identified in field examples as small slip patches within the damage zone (Johnson, 1995; Shipton and Cowie, 2001; Johansen et al., 2005), represents incipient strain softening, fault nucleation, and, perhaps, growth of the "fault core" (Shipton et al., 2005) within the zone (point E on Fig. 3a, step 4 on Figs. 4, 5c). Growth and linkage of slip patches eventually produces a through-going fault that transects the zone (point F on Fig. 3a; step 5 on (Figs. 4, 5d, 1c–e). These slip patches

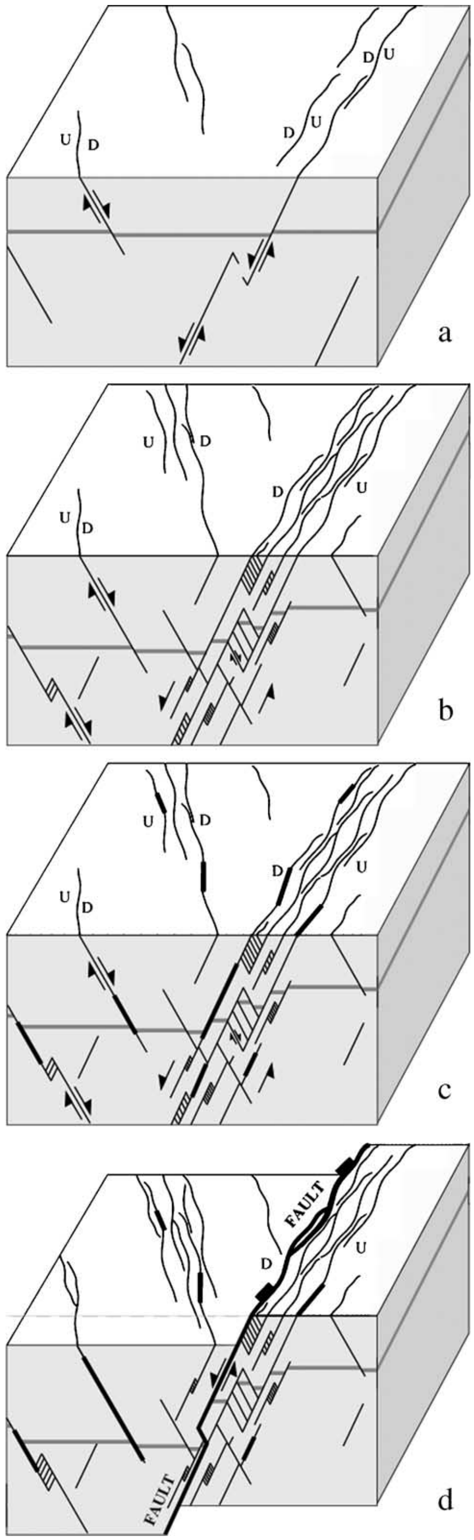

Fig. 5. Synoptic model for the evolution of a faulted array of compaction with shear deformation bands. Thick lines in (c) and (d) represent slip patches superimposed on the earlier-formed bands within the damage zone. D, down; U, up.

and the subsequent fault initially utilize the pre-existing geometry of bands that comprise the damage zone, including corrugations and band segmentation (Schultz and Balasko, 2003; Okubo and Schultz, 2005, in press). These final two stages (steps 4 and 5 on Figs. 4, 5c and d) superimpose a focused strain softening regime onto the formerly distributed strain hardening one (Shipton and Cowie, 2003).

5. Conclusions and outstanding issues

Deformation bands represent yielding in the rock mass, defined here approximately as the transition between elastic, recoverable deformation and permanent, plastic deformation when the localization criteria are met. Faults represent failure, by localized frictional sliding, of bands and damage zones in the host rock. The Cam cap model of yielding in a porous granular geomaterial (soil or rock) provides a useful mechanical framework for understanding how deformation bands grow and eventually fail to form through-going faults. Although experimental work has proved critical to formulating and testing theoretical predictions of band localization, such as from bifurcation theory, systematic study of the associated deformation sequence in natural experiments, as observed in the field, provides additional insight and detail on the sequence and mechanisms to large strains.

The critical state line represents distributed continuum flow at constant volume in a soil; in a porous rock, it simply defines the transition between dilatant and compactional yielding. Surfaces resembling critical state lines in porous rocks are reinterpreted in this paper and identified as either the peak or residual frictional sliding criteria that represent the stress states for which yielded rock (damage zones composed of dilational or compactional deformation bands) changes its deformation style from distributed strain hardening to focused strain softening behavior. Both the individual elements (e.g., bands, cracks) and the total assemblage (e.g., damage zone, large-offset fault zone with linked slip surfaces) must now be considered as "fractures" in the broadest sense of the term.

While many aspects of band formation can be understood by using the Cam cap approach, as modified for porous granular rocks, several aspects invite investigation. Laboratory tests could determine whether the entire yield surface expands as the cap moves outward, potentially making dilational shear bands more difficult to form during unloading from compactional cap conditions, or if the dilational and compactional parts are independent of the loading and deformation sequence. Continued exploration of the differences between localization, yielding, and failure, both in experiments and in field examples, may better define the yield and failure envelopes for porous granular rocks and their evolution with increasing strain in the host rock. Mechanical analysis of propagating deformation bands using criteria such as strain energy density will continue to clarify the geometric development of damage zones and the resulting superimposed fault. Quantitative determination of the paleo-loading paths associated with natural exposures of deformation bands, damage zones, and faulted band networks would significantly advance the understanding of Cam cap-type models as applied to porous-rock deformation.

Acknowledgments

We thank two anonymous referees and journal editor Mike Sandiford for their helpful suggestions that improved the readability of this paper. Discussions with Teng-fong Wong, Kathleen Issen, Haakon Fossen, Scott Wilkins, Chris Okubo, and Chris Wibberley sharpened our focus on yielding vs. failure in porous rocks. Atilla Aydin kindly forwarded a preprint of his recent review paper in JSG. This work was supported by grants from NASA's Planetary Geology and Geophysics Program and NASA's Mars Data Analysis Program (to RAS).

References

Antonellini, M., Aydin, A., 1995. Effect of faulting on fluid flow in porous sandstones: geometry and spatial distribution. American Association of Petroleum Geologists Bulletin 79, 642–671.

Antonellini, M., Pollard, D.D., 1995. Distinct element modeling of deformation bands in sandstone. Journal of Structural Geology 17, 1165–1182.

Antonellini, M., Aydin, A., Pollard, D.D., 1994. Microstructure of deformation bands in porous sandstones at Arches National Park, Utah. Journal of Structural Geology 16, 941–959.

Aydin, A., 1978. Small faults formed as deformation bands in sandstone. Pure and Applied Geophysics 116, 913–930.

Aydin, A., 2000. Fractures, faults, and hydrocarbon entrapment, migration and flow. Marine and Petroleum Geology 17, 797–814.

Aydin, A., Johnson, A., 1978. Development of faults as zones of deformation bands and as slip surfaces in sandstone. Pure and Applied Geophysics 116, 931–942.

Aydin, A., Johnson, A., 1983. Analysis of faulting in porous sandstones. Journal of Structural Geology 5, 19–31.

Aydin, A., Reches, Z., 1982. Number and orientation of fault sets in the field and in experiments. Geology 10, 107–112.

Aydin, A., Borja, R.I., Eichhubl, P., in press. Geological and mathematical framework for failure modes in granular rock. Journal of Structural Geology.

Bartlett, W.L., Friedman, M., Logan, J.M., 1981. Experimental folding and faulting of rocks under confining pressure: Part IX. Wrench faults in limestone layers. Tectonophysics 79, 255–277.

Baud, P., Klein, E., Wong, T.-f., 2004. Compaction localization in porous sandstones: spatial evolution of damage and acoustic emission activity. Journal of Structural Geology 26, 603–624.

Bésuelle, P., 2001a. Compacting and dilating shear bands in porous rock: theoretical and experimental conditions. Journal of Geophysical Research 106, 13435–13442.

Bésuelle, P., 2001b. Evolution of strain localisation with stress in a sandstone: brittle and semi-brittle regimes. Physics and Chemistry of the Earth (A) 26, 101–106.

Bésuelle, P., Rudnicki, J.W., 2004. Localization: shear bands and compaction bands. In: Guéguen, Y., Boutéca, M. (Eds.), Mechanics of Fluid-Saturated Rocks. Elsevier, Amsterdam, pp. 219–321.

Borja, R.I., 2002. Bifurcation of elastoplastic solids to shear band mode at finite strain. Computer Methods in Applied Mechanical Engineering 191, 5287–5314.

Borja, R.I., 2004. Computational modeling of deformation bands in granular media: II. Numerical simulations. Computer Methods in Applied Mechanical Engineering 193, 2699–2718.

Borja, R.I., Aydin, A., 2004. Computational modeling of deformation bands in granular media: I. Geological and mathematical framework. Computer Methods in Applied Mechanical Engineering 193, 2667–2698.

Byerlee, J.D., 1978. Friction of rocks. Pure and Applied Geophysics 116, 615–626.

Byerlee, J.D., Brace, W.F., 1969. High pressure mechanical instability in rocks. Science 164, 713–715.

Challa, V., Issen, K.A., 2004. Conditions for compaction band formation in porous rock using a two yield surface model. Journal of Engineering Mechanics 130, 1089–1097.

Cowie, P.A., Shipton, Z.K., 1998. Fault tip displacement gradients and process zone dimensions. Journal of Structural Geology 20, 983–997.

Crawford, B.R., 1998. Experimental fault sealing: shear band permeability dependency on cataclastic fault gouge characteristics. In: Coward, M.P., Daltaban, T.S., Johnson, H. (Eds.), Structural Geology in Reservoir Characterization, Geological Society of London Special Publication, vol. 127, pp. 27–47.
Crider, J.G., Peacock, D.C.P., 2004. Initiation of brittle faults in the upper crust: a review of field observations. Journal of Structural Geology 26, 691–707.
Crouch, S.L., Starfield, A.M., 1983. Boundary Element Methods in Solid Mechanics. George Allen and Unwin, London.
Cuss, R.J., Rutter, E.H., Holloway, R.F., 2003. The application of critical state soil mechanics to the mechanical behaviour of porous sandstones. International Journal of Rock Mechanics and Mining Sciences 40, 847–862.
Davatzes, N.C., Eichhubl, P., Aydin, A., 2005. Structural evolution of fault zones in sandstone by multiple deformation mechanisms: Moab Fault, southeast Utah. Geological Society of America Bulletin 117, 135–148.
Davis, G.H., 1999. Structural geology of the Colorado plateau region of southern Utah, with special emphasis on deformation bands. Geological Society of America Special Paper, vol. 342. 157 pp.
Davis, R.O., Selvadurai, A.P.S., 2002. Plasticity and Geomechanics. Cambridge University Press, Cambridge.
Davis, G.H., Bump, A.P., García, P.E., Ahlgren, S.G., 2000. Conjugate Riedel deformation band shear zones. Journal of Structural Geology 22, 169–190.
DiMaggio, F.L., Sandler, I.S., 1971. Material model for granular soils. Journal of Engineering Mechanics Div. ASCE 97, 935–950.
Du, Y., Aydin, A., 1993. The maximum distortional strain energy density criterion for shear fracture propagation with applications to the growth of en échelon faults. Geophysical Research Letters 20, 1091–1094.
Du Bernard, X., Eichhubl, P., Aydin, A., 2002. Dilation bands: a new form of localized failure in granular media. Geophysical Research Letters 29, 2176. doi:10.1029/2002GL015966.
Evans, J.P., Bradbury, K.K., 2004. Faulting and fracturing of nonwelded Bishop tuff, eastern California: deformation mechanisms in very porous materials in the vadose zone. Vadose Zone Journal 3, 602–623.
Evans, B., Kohlstedt, D.L., 1995. Rheology of rocks. In: Ahrens, T.J. (Ed.), Rock Physics and Phase Relations—a Handbook of Physical Constants, American Geophysical Union Reference Shelf, vol. 3, pp. 148–165.
Farmer, I.W., 1983. Engineering Behaviour Of Rocks, 2nd. ed. Chapman and Hall, London.
Fisher, Q.J., Casey, M., Harris, S.D., Knipe, R.J., 2003. Fluid-flow properties of faults in sandstone: the importance of temperature history. Geology 31, 965–968.
Flodin, E., Aydin, A., 2004. Faults with asymmetric damage zones in sandstone, Valley of Fire State Park, southern Nevada. Journal of Structural Geology 26, 983–988.
Fossen, H., 2000. Strukturgeologisk ekskursjonguide til Coloradoplatået G-300, våren 2000 (in Norwegian), unpublished field guide. 37 pp.
Fossen, H., Hesthammer, J., 1997. Geometric analysis and scaling relations of deformation bands in porous sandstone. Journal of Structural Geology 19, 1479–1493.
Fossen, H., Hesthammer, J., 1998. Deformation bands and their significance in porous sandstone reservoirs. First Break 16, 21–25.
Fossen, H., Hesthammer, J., 2000. Possible absence of small faults in the Gullfaks Field, northern North Sea: implications for downscaling of faults in some porous sandstones. Journal of Structural Geology 22, 851–863.
Fredrich, J.T., Evans, B., Wong, T.-f., 1989. Micromechanics of the brittle to plastic transition in Carrara marble. Journal of Geophysical Research 94, 4129–4145.
Goodman, R.E., 1989. Introduction to Rock Mechanics, 2nd. ed. Wiley, New York.
Gu, Y., Wong, T.-f., 1994. Development of shear localization in simulated quartz gouge: effect of cumulative slip and gouge particle size. Pure and Applied Geophysics 143, 387–423.
Hill, R., 1950. The Mathematical Theory of Plasticity. Oxford Engineering Science Seris, Oxford, London.
Holcomb, D.J., Olsson, W.A., 2003. Compaction localization and fluid flow. Journal of Geophysical Research 108. doi:10.1029/2001JB000813 (#2290).
Horii, H., Nemat-Nasser, S., 1985. Compression-induced microcrack growth in brittle solids: axial splitting and shear failure. Journal of Geophysical Research 90, 3105–3125.
Issen, K.A., 2002. The influence of constitutive models on localization conditions for porous rock. Engineering Fracture Mechanics 69, 1891–1906.
Issen, K.A., Challa, V., 2003. Conditions for dilation band formation in granular materials. Proceedings of the ASCE Engineering Mechanics Conference 16th, pp. 1–4.
Issen, K.A., Rudnicki, J.W., 2000. Conditions for compaction bands in porous rock. Journal of Geophysical Research 105, 21,529–21,536.
Issen, K.A., Rudnicki, J.W., 2001. Theory of compaction bands in porous rock. Physics and Chemistry of the Earth (A) 26, 95–100.
Jaeger, J.C., 1969. Elasticity, Fracture and Flow. Chapman and Hall, London.
Jaeger, J.C., Cook, N.G.W., 1979. Fundamentals of Rock Mechanics, 3rd ed. Chapman and Hall, New York. 593 pp.
Jamison, W.R., Stearns, D.W., 1982. Tectonic deformation of Wingate sandstone, Colorado National Monument. American Association of Petroleum Geologists Bulletin 66, 2584–2608.
Johansen, T.E.S., Fossen, H., Kluge, R., 2005. The impact of synfaulting porosity reduction on damage zone architecture in porous sandstone: an outcrop example from the Moab Fault, Utah. Journal of Structural Geology 27, 1469–1485.
Johnson, A.M., 1995. Orientations of faults determined by premonitory shear zones. Tectonophysics 247, 161–238.
Johnson, A., 2001. Propagation of deformation bands in porous sandstones. Unpublished course notes, Purdue University (Published online at: http://www.eas.purdue.edu/physproc/pdf%20Files/PropagationofAtillaFaults.pdf).
Khan, A.S., Xiang, Y., Huang, S., 1991. Behavior of Berea sandstone under confining pressure: Part 1. Yield and failure sur-

faces, and nonlinear elastic response. International Journal of Plasticity 7, 607–624.
Kim, Y.-S., Peacock, D.C.P., Sanderson, D.J., 2004. Fault damage zones. Journal of Structural Geology 26, 503–517.
Lockner, D.A., 1995. Rock failure. In: Ahrens, T.J. (Ed.), Rock Physics and Phase Relations —a Handbook of Physical Constants, American Geophysical Union Reference Shelf, vol. 3, pp. 127–147.
Lockner, D.A., Byerlee, J.D., Kuksenko, V., Ponomarev, A., Sidorin, A., 1991. Quasi-static fault growth and shear fracture energy in granite. Nature 350, 39–42.
Mair, K., Main, I., Elphick, S., 2000. Sequential growth of deformation bands in the laboratory. Journal of Structural Geology 22, 25–42.
Mair, K., Frye, K.M., Marone, C., 2002. Influence of grain characteristics on the friction of granular shear zones. Journal of Geophysical Research 107, 2219. doi:10.1029/2001JB000516.
Maltman, A.J., 1984. On the term 'soft-sediment deformation'. Journal of Structural Geology 6, 589–592.
Maltman, A.J., 1988. The importance of shear zones in naturally deformed wet sediments. Tectonophysics 145, 163–175.
Maltman, A.J., 1994. Prelithification deformation. In: Hancock, P.L. (Ed.), Continental Deformation. Pergamon, New York, pp. 143–158.
Marone, C., 1995. Fault zone strength and failure criteria. Geophysical Research Letters 22, 723–726.
Martel, S.J., Pollard, D.D., 1989. Mechanics of slip and fracture along small faults and simple strike-slip fault zones in granitic rock. Journal of Geophysical Research 94, 9417–9428.
Menéndez, B., Zhu, W., Wong, T.f., 1996. Micromechanics of brittle faulting and cataclastic flow in Berea sandstone. Journal of Structural Geology 18, 1–16.
Mollema, P.N., Antonellini, M.A., 1996. Compaction bands: a structural analog for anti-mode I cracks in aeolian sandstone. Tectonophysics 267, 209–228.
Moore, D.E., Lockner, D.A., 1995. The role of microcracking in shear-fracture propagation in granite. Journal of Structural Geology 17, 95–114.
Muir Wood, D.M., 1990. Soil Behaviour and Critical State Soil Mechanics. Cambridge, New York. 462 pp.
Nemat-Nasser, S., Horii, H., 1982. Compression-induced nonplanar crack extension with applications to splitting, exfoliation, and rockburst. Journal of Geophysical Research 87, 6805–6821.
Nova, R., Lagioia, R., 2000. Soft rocks: behaviour and modeling. In: Barla, G. (Ed.), Eurock '96, Prediction and Performance in Rock Mechanics and Rock Engineering, Proceedings of the International Society of Rock Mechanics Symposium, vol. 3. Balkema, Rotterdam, pp. 1521–1540.
Okubo, C.H., Schultz, R.A., 2005. Evolution of damage zone geometry and intensity in porous sandstone: insight gained from strain energy density. Journal of the Geological Society 162 (6), 939–950.
Okubo, C.H., Schultz, R.A., in press. Near-tip stress rotation and the development of deformation band stepover geometries in mode II. Geological Society of America Bulletin.
Okubo, C.H., Schultz, R.A., submitted for publication. Determination of critical strain energy densities for localized plastic yielding in porous sandstone, International Journal of Rock Mechanics and Mining Sciences.
Olsson, W.A., 1999. Theoretical and experimental investigation of compaction bands in porous rock. Journal of Geophysical Research 104, 7219–7228.
Olsson, W.A., 2001. Quasi-static propagation of compaction fronts in porous rock. Mechanics of Materials 33, 659–668.
Olsson, W.A., Holcomb, D.J., 2000. Compaction localization in porous rock. Geophysical Research Letters 27, 3537–3540.
Papamichos, E., Vardoulakis, I., 1995. Shear band formation in sand according to non-coaxial plasticity model. Géotechnique 45, 649–661.
Perić, D., Ayari, M.A., 2002a. Influence of Lode's angle on the pore pressure in generation soils. International Journal of Plasticity 18, 1039–1059.
Perić, D., Ayari, M.A., 2002b. On the analytical solutions for the three-invariant Cam clay model. International Journal of Plasticity 18, 1061–1082.
Petit, J.P., Barquins, M., 1988. Can natural faults propagate under mode-II conditions? Tectonics 7, 1243–1256.
Pollard, D.D., Aydin, A., 1988. Progress in understanding jointing over the past century. Geological Society of America Bulletin 100, 1181–1204.
Pollard, D.D., Segall, P., 1987. Theoretical displacements and stresses near fractures in rock: with applications to faults, joints, veins, dikes, and solution surfaces. In: Atkinson, B.K. (Ed.), Fracture Mechanics of Rock. Academic, New York, pp. 277–349.
Reches, Z., Lockner, D.A., 1994. Nucleation and growth of faults in brittle rocks. Journal of Geophysical Research 99, 18,159–18,173.
Risnes, R., 2001. Deformation and yield in high porosity outcrop chalk. Physics and Chemistry of the Earth 26, 53–57.
Roscoe, K.H., Burland, J.B., 1968. On the generalized stress–strain behaviour of 'wet' clay. In: Heyman, J., Leckie, F.A. (Eds.), Engineering Plasticity. Cambridge University Press, pp. 535–609.
Roscoe, K.H., Poorooshasb, H.B., 1963. A theoretical and experimental study of strains in triaxial tests on normally consolidated clays. Géotechnique 13, 12–38.
Roscoe, K.H., Schofield, A.N., Thurairajah, A., 1963. Yielding of clays in states wetter than critical. Géotechnique 13, 211–240.
Roscoe, K.H., Schofield, A.N., Wroth, C.P., 1958. On the yielding of soils. Géotechnique 8, 22–53.
Rudnicki, J.W., 1977. The inception of faulting in a rock mass with a weakened zone. Journal of Geophysical Research 82, 844–854 (Correction, Journal of Geophysical Research 82, 3437).
Rudnicki, J.W., Rice, J.R., 1975. Conditions for the localization of deformation in pressure-sensitive dilatant materials. Journal of the Mechanics and Physics of Solids 23, 371–394.
Saada, A.S., Liang, L., Figueroa, J.L., Cope, C.T., 1999. Bifurcation and shear band propagation in sands. Géotechnique 49, 367–385.
Schofield, A., Wroth, P., 1968. Critical State Soil Mechanics. McGraw-Hill, New York. 310 pp.
Schultz, R.A., in press. Fractures in Rock: a Field Guide and Journey into Geologic Fracture Mechanics, Oxford University Press.

Schultz, R.A., Fossen, H., 2002. Displacement-length scaling in three dimensions: the importance of aspect ratio and application to deformation bands. Journal of Structural Geology 24, 1389–1411.

Schultz, R.A., Balasko, C.M., 2003. Growth of deformation bands into echelon and ladder geometries. Geophysical Research Letters 30, 2033. doi:10.1029/2003GL018449.

Segall, P., Pollard, D.D., 1983a. Joint formation in granitic rock of the Sierra Nevada. Geological Society of America Bulletin 94, 563–575.

Segall, P., Pollard, D.D., 1983b. Nucleation and growth of strike-slip faults in granite. Journal of Geophysical Research 88, 555–568.

Shipton, Z.K., Cowie, P.A., 2001. Damage zone and slip-surface evolution over μm to km scales in high-porosity Navajo sandstone, Utah. Journal of Structural Geology 23, 1825–1844.

Shipton, Z.K, Cowie, P.A., 2003. A conceptual model for the origin of fault damage zone structures in high-porosity sandstone. Journal of Structural Geology 25, 333–344 (erratum, Journal of Structural Geology 25, 1343–1345).

Shipton, Z.K., Evans, J.P., Robeson, K., Forster, C.B., Snelgrove, S., 2002. Structural heterogeneity and permeability in faulted eolian sandstone: implications for subsurface modelling of faults. American Association of Petroleum Geologists Bulletin 86, 863–883.

Shipton, Z.K., Evans, J.P., Thompson, L.B., 2005. The geometry and thickness of deformation-band fault core and its influence on sealing characteristics of deformation-band fault zones. In: Sorkhabi, R., Tsuji, Y. (Eds.), Faults, Fluid Flow, and Petroleum Traps, American Association of Petroleum Geologists Memoir, vol. 85, pp. 181–195.

Sibson, R.H., 1994. An assessment of field evidence for 'Byerlee' friction. Pure and Applied Geophysics 142, 645–662.

Suppe, J., 1985. Principles of Structural Geology. Prentice-Hall, Englewood Cliffs, New Jersey.

Tapponier, P., Brace, W.F., 1976. Development of stress-induced microcracks in Westerly granite. International Journal of Rock Mechanics and Mining Sciences & Geomechanics Abstracts 13, 103–112.

Vajdova, V., Wong, T.-f., 2003. Incremental propagation of discrete compaction bands: acoustic emission and microstructural observations on circumferentially notched samples of Bentheim sandstone. Geophysical Research Letters 30, 1775. doi:10.1029/2003GL017750.

Vajdova, V., Baud, P., Wong, T.f., 2004a. Compaction, dilatancy, and failure in porous carbonate rocks. Journal of Geophysical Research 109, B05204. doi:10.1029/2003JB002508.

Vajdova, V., Baud, P., Wong, T.f., 2004b. Permeability evolution during localized deformation in Bentheim sandstone. Journal of Geophysical Research 109, B10406. doi:10.1029/2003JB002942.

Vermeer, P.A., de Borst, R., 1984. Non-associated plasticity for soils, concrete, and rock. Heron 29, 3–64.

Wibberley, C.A.J., Petit, J.-P., Rives, T., 1999. Mechanics of high displacement gradient faulting prior to lithification. Journal of Structural Geology 21, 251–257.

Wibberley, C.A.J., Petit, J.-P., Rives, T., 2000. Mechanics of cataclastic 'deformation band' faulting in high-porosity sandstone, Provence. Comptes Rendus de l'Academie de Sciences, Paris 331, 419–425 (in French and English).

Wibberley, C.A.J., Petit, J.-P., Rives, T., in press. The mechanics of fault distribution and localization in high-porosity sands, Provence, France. Journal of the Geological Society of London.

Wilson, J.E., Goodwin, L.B., Lewis, C.J., 2003. Deformation bands in nonwelded ignimbrites: petrophysical controls on fault-zone deformation and evidence of preferential fluid flow. Geology 31, 837–840.

Wolf, H., König, D., Triantafyllidis, T., 2003. Experimental investigation of shear band patterns in granular material. Journal of Structural Geology 25, 1229–1240.

Wong, T.-f., 1982. Shear fracture energy of Westerly granite from post-failure behavior. Journal of Geophysical Research 87, 990–1000.

Wong, T.-f., Baud, P., 1999. Mechanical compaction of porous sandstone. Oil and Gas Science and Technology — Rev. IFP 54, 715–727.

Wong, T.-f., Szeto, H., Zhang, J., 1992. Effect of loading path and porosity on the failure mode of porous rocks. In: Li, V.C. (Ed.), Micromechanical Modelling of Quasi-Brittle Materials Behavior, Applied Mechanics Reviews, vol. 45, pp. 281–293.

Wong, T.-f., David, C., Zhu, W., 1997. The transition from brittle faulting to cataclastic flow in porous sandstones: mechanical deformation. Journal of Geophysical Research 102, 3009–3025.

Wong, T.-f., Baud, P., Klein, E., 2001. Localized failure modes in a compactant porous rock. Geophysical Research Letters 28, 2521–2524.

Wong, T.-f., David, C., Menéndez, B., 2004. Mechanical compaction. In: Guéguen, Y., Boutéca, M. (Eds.), Mechanics of Fluid-Saturated Rocks. Elsevier, Amsterdam, pp. 55–114.

Zhang, J., Wong, T.-f., Davis, D.M., 1990. Micromechanics of pressure-induced grain crushing in porous rocks. Journal of Geophysical Research 95, 341–352.

Zhu, W., Wong, T.-f., 1997. The transition from brittle faulting to cataclastic flow: permeability evolution. Journal of Geophysical Research 102, 3027–3041.